Astron. Astrophys. 299, 755–769 (1995)

ASTRONOMY AND ASTROPHYSICS

Stellar evolution of low- and intermediate-mass stars

II. Post-AGB evolution*

T. Blöcker**

Astrophysikalisches Institut Potsdam, Telegrafenberg A27, D-14473 Potsdam, Germany
e-mail: tbloecker@aip.de

Received 6 July 1994 / Accepted 10 December 1994

Abstract. We present a set of evolutionary tracks for central stars of planetary nebulae in the range from 0.53 to $0.94 M_{\odot}$. These models are based on extensive stellar evolution calculations for initial masses between 1 and $7 M_{\odot}$ which have been carried out all the way from the main sequence through the AGB towards the stage of white dwarfs.

Concerning mass losses during the post-AGB evolution we smoothly reduced the high AGB mass-loss rates and then applied rates adapted from the radiation driven wind theory. The transition time from the AGB to the central-star region depends strongly on the treatment of mass-loss beyond the AGB.

Furthermore, our calculations indicate that massive central stars can fade much more slowly than hitherto assumed. It is shown that the fading time scales and the AGB history are closely connected, and that therefore the preceding mass loss on the AGB plays an important role for the post-AGB evolution.

Key words: stars: evolution – stars: mass loss – stars: AGB, post-AGB – stars: white dwarfs

1. Introduction

Since the pioneering work of Paczyński (1970, 1971) it seemed to be quite safe to state that the evolution of post-AGB models, i.e. their evolutionary speed, depends only on their core mass $M_{\rm H}$ ($\approx$ remnant mass) (and the thermal-pulse cycle phase ϕ with which the models leave the AGB). Schönberner's (1979, 1983) calculations for low and moderate-mass post-AGB models indicated that the consideration of mass loss affects the evolutionary speed only in the vicinity of the AGB, i.e. for $T_{\rm eff} < 10000$K. The calculations of Wood & Faulkner (1986) (based on the AGB calculations of Wood & Zarro 1981) for moderate to high-mass models confirmed the results of Paczyński (1970, 1971) that the fading time decreases with increasing remnant mass. But in 1990 Blöcker & Schönberner pointed out that not only the remnant mass but also the initial mass, and thus the history of the models, determines the fading timescales. They demonstrate that only a proper treatment of the preceding AGB evolution and combinations of initial and final masses which are consistent with empirical initial-final mass relationships yield reliable timescales. Their massive remnant of $0.84 M_{\odot}$ fades *slower* than a less massive one of $0.61 M_{\odot}$. This is in contrast to the results of former calculations. But both the models of Paczyński (1970, 1971) and of Wood & Faulkner (1986) are based on just one initial mass, namely on a $3 M_{\odot}$ and a $2 M_{\odot}$ star, resp., leading to inconsistent combinations of initial and final masses for more massive models. Later on, Blöcker (1993a, 1993b) demonstrated that the post-AGB evolution of two massive models of *equal* remnant mass ($0.84 M_{\odot}$) but *different* initial masses (3 and $5 M_{\odot}$, resp.) gives completely different fading timescales due to the different internal structure of the models. This stresses the importance of a consistent treatment of the AGB evolution for post-AGB timescales.

Recently, Vassiliadis & Wood (1994) presented a new set of evolutionary post-AGB tracks. Their models are based on the AGB calculations of Vassiliadis & Wood (1993). The corresponding final masses agree with the empirical relationship of Weidemann (1987) within $\approx 0.1 M_{\odot}$. Vassiliadis & Wood (1994) found (like Paczyński 1971 and Wood & Faulkner 1986) that the higher the central-star mass, the lower is the luminosity on the fading part at an post-AGB age of $\approx 10^4$yrs, conflicting again with the results of Blöcker & Schönberner (1990). They stated that "the reasons for different evolutionary rates at a given core mass requires further study".

Based on our AGB models presented in the first part of this series (Blöcker 1994) we continue our studies of the consequences of different mass-loss histories for the post-AGB evolution. By means of a set of evolutionary post-AGB calculations we will show how sensitively the fading time scales of especially more massive remnants depend on the duration of the preceding AGB evolution, i.e. on the applied mass-loss law. In Blöcker

* Tables 3,4 and 5 are only available in electronic form at the CDS via ftp 130.79.128.5

** *Former address:* Institut für Astronomie und Astrophysik, D-24098 Kiel, Germany

(1994) we derived an AGB mass-loss law from the dynamical calculations of Bowen (1988) yielding final masses which are consistent with the observed initial-final mass relationship over the whole mass range. Taking such a mass-law into account we will show that, indeed, massive remnants can fade slower than low-mass ones.

This paper is organized as follows: After a brief decription of some computational details (Sect. 2) we summarize the evolution towards and along the AGB mainly with respect to mass loss in Sect. 3. The way how we have treated mass loss beyond the AGB is described in Sect. 4. Then, the post-AGB evolution of hydrogen (Sect. 5.1) and helium burning models (Sect. 5.2) is presented. Finally, we give some conclusions in Sect. 6.

2. Computational details

All calculations are based on the well-known Kippenhahn code in a widely modified and extended version of Schönberner's (1983) adaption (cf. Blöcker 1993a). We calculated the evolution of 1, 3, 4, 5 and $7 M_{\odot}$ stars from the zero age main sequence (ZAMS) through the AGB towards the stage of white dwarfs. The initial composition was $(X, Y, Z) = (0.739, 0.24, 0.021)$.

Mass loss was considered since the beginning of the RGB. We followed for all initial masses the evolution to the stage of white dwarfs with a common treatment of mass loss composed of different descriptions for the RGB, AGB and post-AGB phase. Additionally, we calculated also some AGB sequences with other mass-loss formulae. Beyond the AGB we considered mass-loss rates given by the radiation-driven wind theory of Pauldrach et al. (1988). Furthermore, we take a smooth transition from the high AGB mass loss to the orders of magnitude weaker central-star wind into account. For more details see Blöcker (1994).

3. The evolution towards and along the AGB

Since our treatment of mass loss along the AGB is discussed in detail by Blöcker (1994) we give here only a brief summary. In the following formulae the stellar luminosity L, radius R and mass M are always given in solar units.

On the RGB and during the stage of central helium burning we calculated mass loss according to Reimers (1975):

$$\dot{M}_{\rm R} = 4 \cdot 10^{-13}\, \eta_{\rm R} \frac{LR}{M} \qquad [M_{\odot}/\mathrm{yr}]. \tag{1}$$

Concerning the $1 M_{\odot}$ sequence we chose on the RGB $\eta_{\rm R} = 0.5$ (cf. Maeder & Meynet 1989). Due to its long life time on the RGB the total mass loss amounted to $\approx 0.3 M_{\odot}$. During central helium burning (with $\eta_{\rm R} = 1$) mass loss is much smaller (1.2% of the initial mass) since the corresponding luminosities are considerably smaller.

For all other models (3, 4, 5 and $7 M_{\odot}$) we had always set $\eta_{\rm R} = 1$. Here, mass loss on the RGB is not important, the models lost only 1-3% of their initial masses until they reached the AGB.

On the AGB when dust formation becomes important the Reimers (1975) rate is not applicable any longer since it cannot

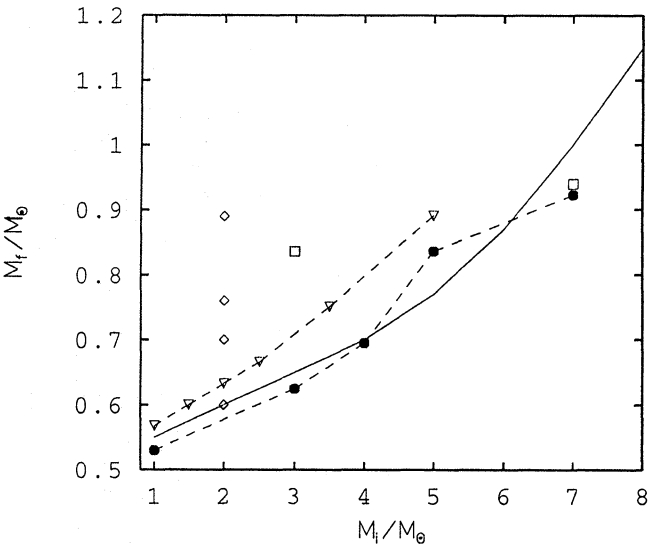

Fig. 1. Final mass vs. initial mass for different mass-loss histories on the AGB. The solid line is the initial-final mass relationship of Weidemann (1987). The symbols mean:
- • Blöcker (1994): Bowen-like mass loss $\dot{M}_{\rm B1}$
- □ special treatment (e.g. $\dot{M}_{\rm BH}$ + superwind)
- ◇ Wood & Faulkner (1986)
- ▽ Vassiliadis & Wood (1993)

reproduce the strong increase of mass loss. We adapted the numerical results of Bowen (1988) which are based on dynamical models for atmospheres of Mira-like stars. Taking his standard model with the inclusion of dust we got:

$$\dot{M}_{\rm B1} = 4.83 \cdot 10^{-9}\, M_{\rm ZAMS}^{-2.1} \cdot L^{2.7} \cdot \dot{M}_{\rm R} \qquad [M_{\odot}/\mathrm{yr}] \tag{2}$$

For pulsational periods P_0 (fundamental mode) less than 100 d we further used the Reimers rate since it gives still reasonable rates for low periods. For larger periods a Bowen-like mass-loss was applied. The periods P_0 had been calculated according to Ostlie & Cox (1986):

$$\log(P_0/\mathrm{d}) = -1.92 - 0.73 \log M + 1.86 \log R. \tag{3}$$

We want to remind that the relation $\dot{M}_{\rm B1} \sim L^{2.7} \cdot \dot{M}_{\rm R}$ has been directly derived from Bowen's (1988) models. The term $4.83 \cdot 10^{-9} M_{\rm ZAMS}^{-2.1}$ has been introduced in order to provide a smooth transition between a Reimers- and a Bowen-like mass loss at $P_0 = 100$ d. Regarding that term the actual stellar mass at the transition point can be approximated by the initial mass for $M_{\rm ZAMS} > 2 M_{\odot}$. For more details see Blöcker (1994).

With this mass-loss description we calculated the AGB evolution for $M_{\rm ZAMS} = 1$, 3, 4, 5 and $7 M_{\odot}$. Figure 1 shows that the resulting final masses are consistent with the empirical initial-final mass relationship of Weidemann (1987). At the tip of the AGB the respective mass-loss rates amounted up to $\approx 10^{-4} M_{\odot}$/yr. Only in the case of the $1 M_{\odot}$ sequence the mass-loss rates had been considerably smaller ($\approx 10^{-7} M_{\odot}$/yr) since the AGB evolution terminated immediately before reaching the TP-AGB (due to the high total mass loss of $0.3 M_{\odot}$ on the RGB).

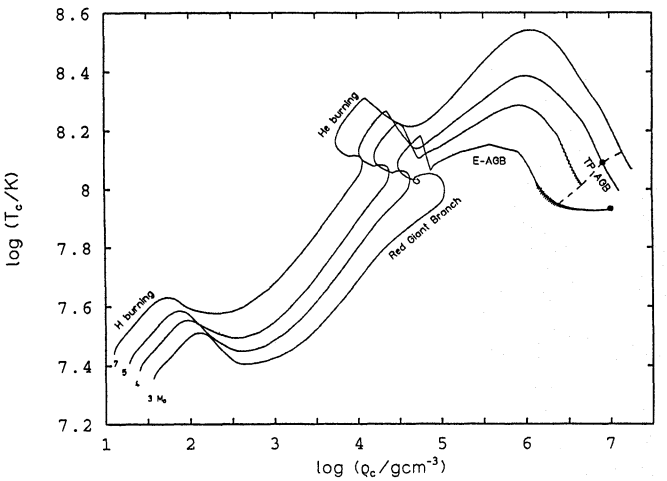

Fig. 2. Evolution of the central values of density and temperature for different sequences. The dashed line indicates the tip of the AGB for sequences calculated with $\dot{M}_{\rm B1}$, the filled dots refer to massive remnants of $0.836M_\odot$

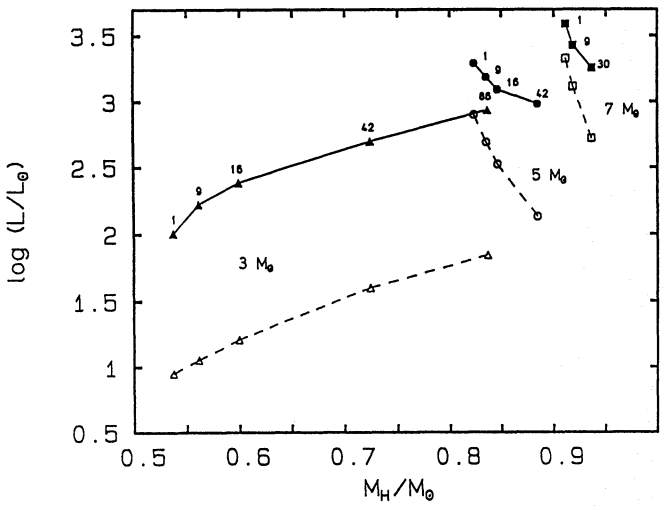

Fig. 3. Evolution of $L_{\rm g}$ (filled symbols) and L_ν (open symbols) along the AGB for three initial masses. The numbers denote selected thermal pulses ($\phi = 0.5$)

At this point P_0 was still below 100 d and the transition from a Reimers to a Bowen-like mass loss was not reached.

We also introduced an even steeper increasing mass-loss rate $\dot{M}_{\rm B2}$ by replacing the initial mass in (2) for the actual stellar mass. However, calculations for $M_{\rm ZAMS} = 3$ and $5M_\odot$ show that the remnant masses differ appreciably only for low initial masses. Additionally, we calculated AGB sequences for $M_{\rm ZAMS} = 3$, 5 and $7M_\odot$ with the mass-loss formula of Baud & Habing (1983), $\dot{M}_{\rm BH}$. However, this rate increases only very slowly along AGB and yields remnant masses which are too large. For instance, the AGB evolution of a $3M_\odot$ progenitor terminated with a final mass of $0.814M_\odot$. (cf. Blöcker 1994)

In order to get two massive AGB remnants with the same final mass ($0.836M_\odot$) but different history, i.e. initial mass (3 and $5M_\odot$, resp.), we split the $3M_\odot$ sequence with $\dot{M} = \dot{M}_{\rm BH}$. For that purpose we set $\dot{M} = 0$ after pulse No. 62 when $(M, M_{\rm H}) = (1.67M_\odot, 0.784M_\odot)$. Then, 24 pulses later, $M_{\rm H} = 0.836M_\odot$ was reached. and a well-timed onset of a constant mass-loss rate of $\dot{M} = 5 \cdot 10^{-4}\,M_\odot$/yr ("superwind", Renzini 1981) terminated the AGB evolution immediately. Looking at Fig. 1 one sees that this remnant mass is, of course, definitely too large for a progenitor of $3M_\odot$. The same is true for the more massive remnants of Wood & Faulkner (1986) which all belong to an inital mass of $2M_\odot$.

We have also split the $7M_\odot$ sequence with $\dot{M} = \dot{M}_{\rm BH}$ in order to get a massive remnant of $0.94M_\odot$. This was done by introducing a constant rate of $\dot{M} = 4 \cdot 10^{-4}\,M_\odot$/yr at pulse No. 26. The AGB evolution terminated 5 pulses later.

Figure 1 shows also the calculations of Vassiliadis & Wood (1993). Their final masses are somewhat larger than our ones and are up to $\approx 0.1M_\odot$ above the observed initial-final relationship of Weidemann (1987).

For the post-AGB evolution we only considered remnants which are consistent with the initial-final mass relationship. Additionally, we have calculated the evolution for the second massive remnant of $0.836M_\odot$ belonging to a $3M_\odot$ progenitor in order to investigate the influence of a different history for cores of equal mass (cf. Blöcker & Schönberner 1990; Blöcker 1993a, 1993c). Some properties of these models are collected in Table 1. One remark has to be made concerning the lifetimes on the E-AGB. Since we used older opacities (Cox & Stewart 1970) and, more important, do not consider semiconvection our convective cores during central helium burning are smaller than those of e.g. Vassiliadis & Wood (1993) for lower initial masses. Correspondingly, the lifetime for central helium burning $t_{\rm HeB}$ is smaller, too. Both lead to an increase of the duration of the E-AGB phase (see e.g. Sweigart et al. 1990). For instance, Vassiliadis & Wood got $t_{\rm HeB} = 1.42 \cdot 10^8$ and $t_{\rm E-AGB} = 1.21 \cdot 10^7$yr for $M_{\rm ZAMS} = 1M_\odot$ whereas we got $6.27 \cdot 10^7$ and $4.46 \cdot 10^7$. The sum of $t_{\rm HeB}$ and t_{E-AGB} differs by only $\approx 30\%$. Therefore, the thermomechanical structure of the hydrogen exhausted cores should be comparable at the first thermal pulse.

Furthermore, we want to recall the evolution in the density-temperature plane shown in Fig. 2 and the evolutionary course of the gravothermal luminosity and the neutrino losses along the TP-AGB illustrated in Fig. 3 (see Blöcker 1994). The following important conclusions can be drawn from these figures: Firstly, mass loss prevents a convergence of the evolutionary lines for central temperatures and densities (see Paczński (1970) for such a convergence). Correspondingly, the respective lines for the mentioned luminosity contributions do not merge either. Secondly, even cores of *equal* mass (e.g. $0.836M_\odot$) can have a completely *different* thermomechanical structure, and the fading part of the post-AGB evolution can be expected to be different, too.

4. Mass loss beyond the AGB

At the tip of the AGB high mass-loss rates of $\approx 10^{-4}M_\odot$/yr or even more are reached and the models begin to leave the AGB

Table 1. Some properties of the models: initial mass, core mass at the tip of the AGB (≈ final mass), lifetime on the E-AGB and TP-AGB, total number of thermal pulses and the used AGB mass-loss law. The signs B1 and B2 refer to the Bowen-like mass-loss $\dot{M}_{B1}$ and $\dot{M}_{B2}$, resp., R to Reimers (1975), BH to Baud and Habing (1983) and SP to a special treatment of mass-loss introduced to get remnants of specified mass ($0.836M_\odot$, $0.94M_\odot$; see text)

$\frac{M_{ZAMS}}{M_\odot}$	$\frac{M_H}{M_\odot}$	$\frac{t_{E-AGB}}{yrs}$	$\frac{t_{TP-AGB}}{yrs}$	N_{TP}	$\dot{M}$
1	0.529	$4.46 \cdot 10^7$	/	/	R
3	0.605	$6.96 \cdot 10^7$	$1.62 \cdot 10^6$	17	B2
	0.625		$1.87 \cdot 10^6$	20	B1
	0.836		$3.26 \cdot 10^6$	86	SP
4	0.696	$1.98 \cdot 10^7$	$4.54 \cdot 10^5$	15	B1
5	0.836	$8.29 \cdot 10^6$	$5.79 \cdot 10^4$	9	B1
7	0.940	$1.71 \cdot 10^6$	$8.50 \cdot 10^4$	31	SP

when the envelope mass drops below several percent of the total mass ($\approx 10^{-2}M_\odot$).

Observations indicate that the mass-loss rates of central stars of planetary nebulae are up to several orders of magnitude below those of the immediately preceding AGB evolution (cf. Perinotto 1989). Therefore, mass-loss has to decrease strongly during the transition between the AGB and the central-star regime.

At the tip of the AGB many stars are hidden by thick dust shells and only the infrared radiation of the circumstellar shell can be observed. However, when the AGB evolution terminates the dust shell becomes optically thin due to its continuous expansion and the decreasing mass loss, and the star "shines through" again. IRAS observations have detected a lot of objects with spectral types F and G which are surrounded by cool (≈ 100 K) and optically thin dust shells (e.g. Parthasarathy & Pottasch 1986; Likkel et al. 1987; Pottasch & Parthasarathy 1988) and are related to this evolutionary stage (Luck & Bond 1984). Typical members of this phase are also the non variable OH/IR stars whose spectra also show clearly separated dust components (cf. Habing et al. 1989). Dust shell calculations of Bedijn (1987) indicate that the mass-loss rates of these objects are orders of magnitude smaller than those at the tip of the AGB, which is also supported by observations (van der Veen et al. 1989).

Since the periods and amplitudes of the radial pulsations are rapidly decreasing during the transition to the central-star regime our adaption of Bowen's (1988) calculations is not applicable any longer. Furthermore, while the model evolves to higher effective temperatures, $\dot{M}_{B1}$ as well as $\dot{M}_R$ decreases with T_{eff}^{-2} because the luminosity remains constant and the final mass is almost reached. Thus, a typical AGB mass-loss of $10^{-4}M_\odot$/yr would only drop by a factor of 7 when T_{eff} increases from 3000 to 8000 K.

Up to now it is not known - neither from observations nor from theory - how and at which temperature (range) the strong decrease of the mass-loss rates takes place. Former calculations like those of Schönberner (1983) and Wood & Faulkner (1986) treated the final AGB evolution with an artifically invoked superwind until a certain temperature was reached (e.g. 5000 and 6300 K, resp.). Then, the Reimers rate was used or mass-loss was even totally switched off.

However, dust shell calculations of Bedijn (1987) for non-variable OH/IR stars indicated that the observed dust shell spectra can be much better modelled by assuming a *non-abrupt* decrease of the mass-loss rates. Therefore, we have reduced the AGB mass-loss rate proportional to the (decreasing) radial pulsational period P_0 (Blöcker 1989; Blöcker & Schönberner 1990) Starting this reduction at P_0 = 100 d the mass-loss rate was stepped down in such a manner that the Reimers' rate was reached at P_0 = 50 d. This point corresponds to our age zero of the central-star evolution. Additionally, we split the sequence $(M_{ZAMS}, M_H) = (3M_\odot, 0.625M_\odot)$ and performed the reduction between 150 and 100 d, too. The formula for the transition rate is given by

$$\dot{M}_{trans} = \dot{M}_{AGB}(t_1) - \Delta\dot{M}(t) \cdot \frac{P_0(t_1) - P_0(t)}{P_0(t_1) - P_0(t_2)} \qquad (4)$$

with $\Delta\dot{M}(t) = \dot{M}_{AGB}(t_1) - \dot{M}_R(t)$.
The times t_1 und t_2 refer to the beginning and the end of the reduction ($t_1 \le t \le t_2$).

Then, the Reimers rate, decreasing with T_{eff}^{-2}, was kept until it dropped beneath the values given by the radiation-driven wind theory according to Pauldrach et al. (1988) which is applicable for effective temperatures greater than, say, 20000 K. Neglecting the slight temperature dependence of their model results we have adapted their mass-loss rates by (cf. Blöcker 1989; Blöcker & Schönberner 1990):

$$\dot{M}_{CPN} = 1.29 \cdot 10^{-15} L^{1.86} \qquad [M_\odot/yr] \qquad (5)$$

This mass-loss law was used for the remaining part of the post-AGB evolution. It provided maximal rates of $1.5 \cdot 10^{-8}$ to $2.1 \cdot 10^{-7}M_\odot$/yr for M_H = 0.6 to $0.94M_\odot$ during the horizontal part of the evolution and yielded quickly decreasing rates along the cooling part.

Table 2 gives the mass-loss rates, temperatures and luminosities at the beginning and the end of the reduction as well at the point where we switched to the results of the radiation-driven wind theory. ϕ is the thermal-pulse phase reached at age zero (P_0 = 50 d and for one $0.625M_\odot$ sequence P_0 = 100 d, resp.). Δt gives the duration of the reduction and t the time with respect to age zero necessary to reach the region where we calculated the mass-loss according to Pauldrach et al. (1988). The reduction time Δt varies from a few to several hundred years. The duration t of the phase during which we used the Reimers (1975) rate (i.e. from P_0 = 50 d until $\dot{M}_{CPN}$ becomes valid) shrinks with increasing core mass, viz. from ≈ 1700 yrs for $0.605M_\odot$ to ≈ 11 yrs for $0.94M_\odot$. This is due to the fact that the burning

Table 2. Mass-loss rates, effective temperatures and luminosities at the beginning and the end of the mass-loss reduction and at the point where we used the results of the radiation-driven wind theory. Δt gives the duration of the mass-loss reduction which was performed between $P_0 = 100$ and 50 d (for $(M_{\rm ZAMS}, M_{\rm H}) = (3M_\odot, 0.625M_\odot)$ additionally between 150 and 100 d). ϕ is the thermal-pulse phase at the end of the reduction corresponding to our age zero of the central-star evolution. B1 and B2 correspond to a Bowen-like mass loss according to $\dot{M}_{\rm B1}$ and $\dot{M}_{\rm B2}$, resp., R to the Reimers rate and CPN to the adapted rates of Pauldrach et al. (1988). t gives the time passed with respect to age zero until $\dot{M}_{\rm CPN}$ becomes valid

$\frac{M_{\rm ZAMS}}{M_\odot}$	$\frac{M_{\rm H}}{M_\odot}$	$\frac{P_0}{\rm d}$	$\frac{\dot{M}}{M_\odot/{\rm yr}^{-1}}$	rate	$\log\frac{T_{\rm eff}}{\rm K}$	$\log\frac{L}{L_\odot}$	$\frac{\Delta t}{\rm yr}$	ϕ	$\frac{t}{\rm yr}$
3	0.605	100	$1.15\cdot10^{-4}$	B2	3.701	3.805			
		50	$3.15\cdot10^{-7}$	R	3.782	3.800	158	0.50	
			$1.50\cdot10^{-8}$	CPN	4.436	3.800			1694
3	0.625	150	$1.45\cdot10^{-5}$	B1	3.687	3.952			
		100	$7.23\cdot10^{-7}$	R	3.724	3.908	2845	0.87	
			$2.31\cdot10^{-8}$	CPN	4.410	3.900			7292
3	0.625	100	$9.33\cdot10^{-6}$	B1	3.725	3.908			
		50	$3.77\cdot10^{-7}$	R	3.805	3.902	778	0.86	
			$2.31\cdot10^{-8}$	CPN	4.408	3.900			666
4	0.696	100	$1.75\cdot10^{-5}$	B1	3.757	4.071			
		50	$4.89\cdot10^{-7}$	R	3.847	4.067	19	0.50	
			$4.72\cdot10^{-8}$	CPN	4.361	4.067			87
5	0.836	100	$4.72\cdot10^{-5}$	B1	3.787	4.256			
		50	$6.89\cdot10^{-7}$	R	3.865	4.243	45	0.44	
			$1.00\cdot10^{-7}$	CPN	4.284	4.242			87
7	0.940	100	$1.00\cdot10^{-3}$	SP	3.816	4.404			
		50	$9.57\cdot10^{-7}$	R	3.900	4.419	0.9	0.50	
			$2.08\cdot10^{-7}$	CPN	4.237	4.413			11

rate $\dot{M}_{\rm H}$, and thus the evolutionary speed, increases and the temperature where $\dot{M}_{\rm R}$ falls below $\dot{M}_{\rm CPN}$ decreases with increasing core mass. The radiation driven winds start at $T_{\rm eff} \approx 27000$ K for $M_{\rm H} = 0.61M_\odot$ and at ≈ 17000 K for $0.94M_\odot$.

The time spans Δt and t considerably increase if the mass-loss reduction is carried out between $P_0 = 150$ d and 100 d instead between 100 d and 50 d. In that case mass loss decreases closer to the AGB leading to an earlier decrease of the evolutionary speed.

Recently, Vassiliadis & Wood (1994) presented a new set of evolutionary post-AGB tracks. They also considered the results of Pauldrach et al. (1988). The high AGB mass losses were stopped by switching to an adaption to the radiation driven wind theory when the model has moved off the AGB by $\Delta \log T_{\rm eff} = 0.3$. This point corresponds to temperatures of less than 5000 K. Since in that scenario the change from AGB to post-AGB mass-loss rates occurs closer to the AGB than in our calculations, and also a reduction phase is missing, the transition times as defined by Vassiliadis & Wood (1994) (= time from minimum temperature at the tip of the AGB + $\Delta \log T_{\rm eff} = 0.3$ until $\log T_{\rm eff} = 4$) are larger than our ones.

Concerning the radiation driven winds they derived a formula which, although based on the same data, differs from our adaption. Taking their formulae (1), (2) and (3) one gets for the horizontal part of the evolution (when the core-mass luminosity relation can be applied) $\dot{M} \sim (L/T_{\rm eff})^{0.75}$. Thus, this prescription leads to a steeper decrease of the mass-loss rates during the plateau evolution and a slower decrease during the fading part than predicted by our adaption. Since Vassiliadis & Wood (1994) assumed a mean mass of $0.6M_\odot$ for all central stars and neglected the Eddington factor Γ (ratio of stellar luminosity to Eddington luminosity) in their derivation their mass-loss law depends weaker on the luminosity than our one. However, the resulting differences of the evolutionary speeds depend on the respective ratio of burning rate to mass-loss rate and are only noticeably for massive remnants (see below).

Regarding hydrogen burning models the following evolutionary time scale can be estimated (cf. Schönberner & Blöcker 1993):

$$\Delta t_{\rm H} \approx \frac{\Delta M_{\rm env}}{\dot{M}_{\rm H} + \dot{M}_{\rm w}} \qquad (6)$$

with $\Delta M_{\rm env} = M_{\rm env}(t_1) - M_{\rm env}(t_2)$ and $t_2 > t_1$. $M_{\rm env}$ is the envelope mass, $\dot{M}_{\rm H}$ the growth rate of the core and $\dot{M}_{\rm w}$ the mass loss close to or beyond the AGB (= $\dot{M}_{\rm AGB}$, $\dot{M}_{\rm trans}$, $\dot{M}_{\rm R}$ and $\dot{M}_{\rm CPN}$, resp.). The evolution of the envelope mass as a function of the effective temperature is shown in Fig. 4. Since $\Delta M_{\rm env}$ decreases and $\dot{M}_{\rm H}$ increases with increasing core mass, more

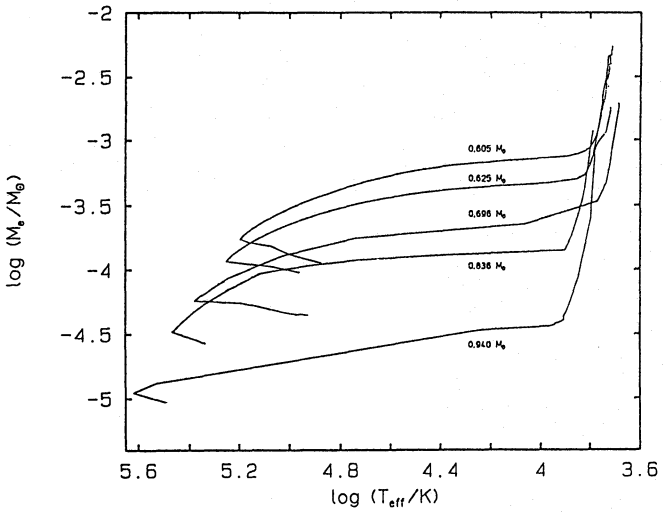

Fig. 4. The envelope mass as a function of the effective temperature for several hydrogen burning models. The labels refer to the respective core masses

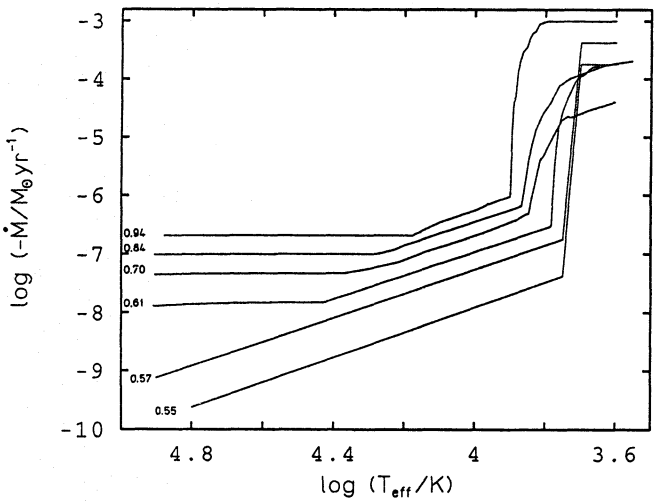

Fig. 5. Mass loss vs. effective temperatures for post-AGB models of 0.605, 0.696, 0.836 and $0.94 M_\odot$, and of $0.546 M_\odot$ and $0.565 M_\odot$ from Schönberner (1983)

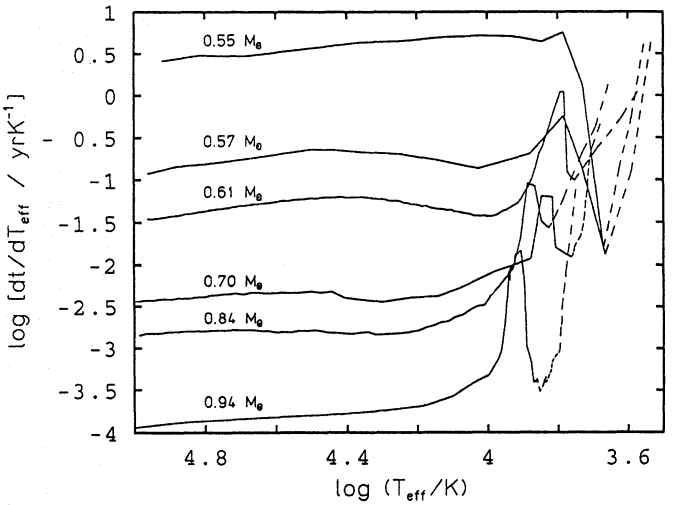

Fig. 6. Reciprocal evolutionary rates vs. effective temperatures for post-AGB models of 0.605, 0.696, 0.836 and $0.94 M_\odot$ and of $0.546 M_\odot$ and $0.565 M_\odot$ from Schönberner (1983). The dashed lines indicate where the respective star is expected to be obscured by dust

massive remnants evolve faster than less massive ones along the horizontal part of the evolution. Mass loss accelerates the evolution somewhat.

The temporal evolution of the mass-loss rates for the whole AGB and reduction phase (between P_0 = 100 and 50 d) has already been illustrated in Blöcker (1994). The post-AGB evolution of the mass loss as a function of the effective temperature along the horizontal part of the evolutionary tracks is shown in Fig. 5 complemented with two low mass models calculated by Schönberner (1983), whereas Fig. 6 presents the respective (reciprocal) evolutionary rates. At low effective temperatures, $T_{\rm eff} < 5000$K, mass loss is large and determines the evolutionary speed, $\dot{T}_{\rm eff}$. Due to the dust component, the star can be expected to be completely obscured (dashed lines). The quick decrease of $\dot{M}$ leads to a corresponding deceleration of the evolution until the evolution speeds up again since $\Delta M_{\rm env}/\Delta T_{\rm eff}$ becomes very small (cf. Fig. 4). Above $\approx$ 16000K, the mass-loss rates of low mass models become unimportant compared to the respective burning rates ($0.6 M_\odot$: $\dot{M}_{\rm w} \approx 0.1 \dot{M}_{\rm H}$). However, the evolution of more massive models is strongly affected by mass loss all the way till the exhaustion of the burning shells. Due to $\dot{M}_{\rm CPN} \sim \dot{M}_{\rm H}^{1.9}$ one gets for the massive remnants of 0.84 and $0.94 M_\odot$ $\dot{M}_{\rm CPN} \approx 0.5 \dot{M}_{\rm H}$. Hence, even for high effective temperatures the evolutionary speed increases by 50% due to mass loss!

In this mass-loss scenario the reciprocal evolutionary rates have their relative maximum between 6000 and 8300 K leading to a higher detection probability of post-AGB stars in this temperature range (cf. Schönberner & Blöcker 1993). Indeed, many post-AGB objects have been observed just in that spectral region. For instance, Parthasarathy (1993) listed 48 post-AGB supergiant like stars detected from IRAS covering spectral types from B5 to M7. From this sample 28 objects are A7 to F9 stars whereas two groups of 10 objects each belong to earlier and later spectral types, respectively. For observational details (identification criteria, data selection, binarity, etc.) see Parthasarathy (1993) and references therein. However, up to now the interpretation of such data should be treated with some caution and it would be worthwile to make more quantitative studies considering all selection effects due to bolometric corrections, scale heights, etc.

5. Central-star tracks

5.1. Hydrogen burning models

The evolutionary tracks for all hydrogen burning sequences consistent with reliable inital-final mass relationships are shown in Fig. 7 ($M_{\rm H}$ = 0.605, 0.625, $0.836 M_\odot$ and Fig. 8 ($M_{\rm H}$ = 0.696,

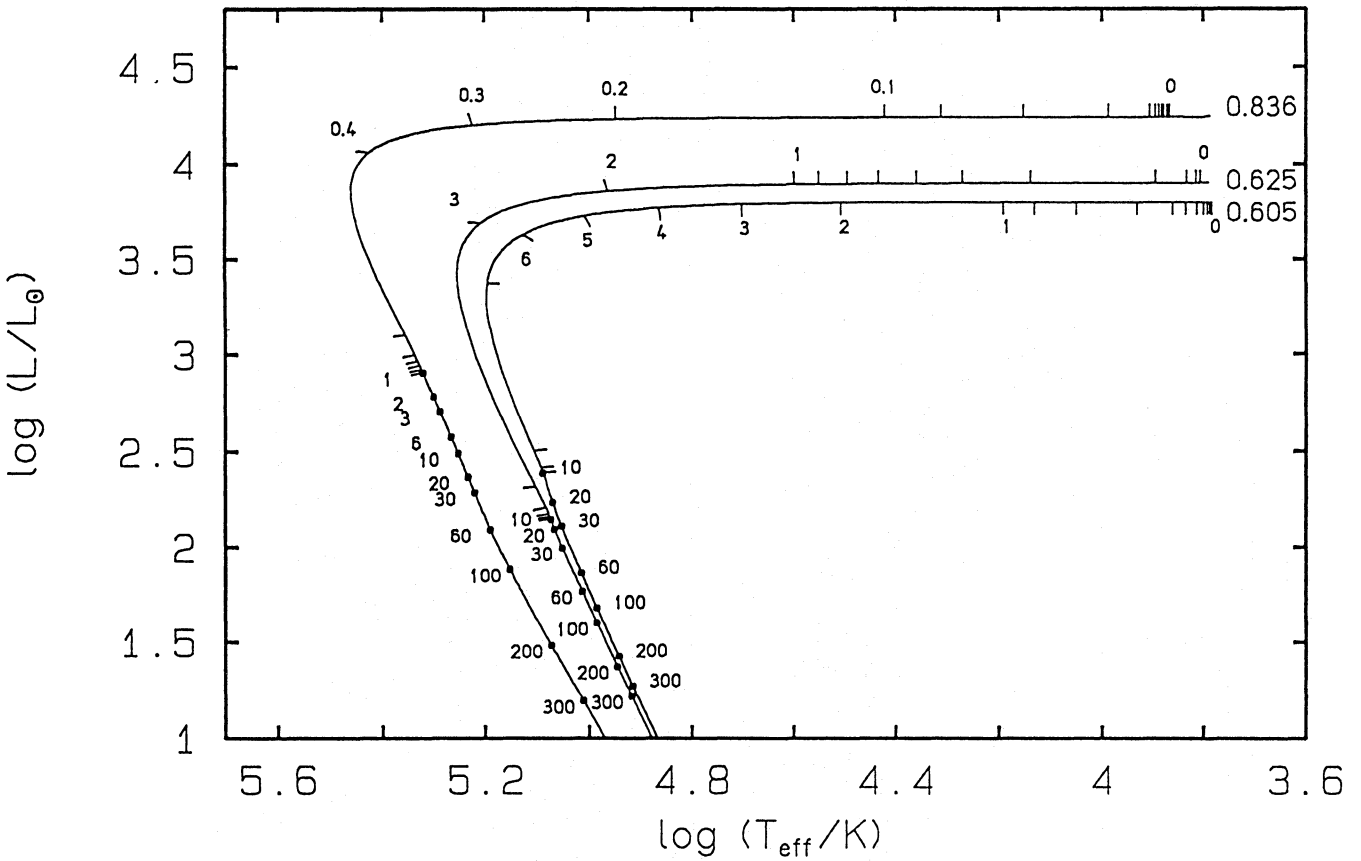

Fig. 7. Evolution of post-AGB models with ($M_{\rm ZAMS}$, $M_{\rm H}$) = ($3M_\odot, 0.605M_\odot$), ($3M_\odot, 0.625M_\odot$) and ($5M_\odot, 0.836M_\odot$). Time marks are in units of 10^3 yrs

$0.940M_\odot$), the corresponding data[1] is given in Table 3 and 4. The time necessary for the whole horizontal part of the evolution ranges from only $\approx$ 60 yrs for the most massive model of $0.94M_\odot$ to several thousand years for the low mass models. The evolutionary speeds are in all cases somewhat higher than those given by Schönberner (1983), Wood & Faulkner (1986) or Vassiliadis & Wood (1994). This is mainly due to the different treatment of mass loss.

Figure 9 shows the luminosity contributions due to hydrogen ($L_{\rm H}$) and helium ($L_{\rm He}$) burning, gravothermal energy releases ($L_{\rm g}$) and neutrino losses (L_ν) as well as the surface luminosity ($L_{\rm sur}$) as a function of time for the sequences shown in Figs. 7 and 8. When nuclear shell burning ceases the surface luminosity rapidly declines by more than one order of magnitude. Then the evolution slows down because the luminosity is mainly determined by gravothermal energy releases and neutrino losses. The onset of the decelaration depends on the value of $L_{\rm g}$ reached at the tip of the AGB. It has already been illustrated in Fig. 3 that the evolution of $L_{\rm g}$ along the AGB depends, in turn, sensitively on both the core mass and the initial mass.

Since Paczyński (1971) had presented the first model calculations of post-AGB remnants it seemed to be quite sure that more massive remnants fade faster than less massive ones. Subsequent calculations of Wood & Faulkner (1986) yielded confirming results. However, our massive model with ($M_{\rm ZAMS}$, $M_{\rm H}$)=($5M_\odot, 0.836M_\odot$) fades *slower* than the low mass one with ($3M_\odot, 0.605M_\odot$)! For instance, at $\log(L/L_\odot)$ = 2.1 the post-AGB age of the consistent $0.836M_\odot$ model amounts to $\approx$ 60000 yrs, being twice as large as the corresponding age of the $0.605M_\odot$ remnant. The more massive models of Wood & Faulkner (1986) reach that age in less than 10000 yrs. These differences are mainly due to the different treatment of the preceding AGB evolution, i.e. of the history of the models (cf. Blöcker & Schönberner 1990).

To demonstrate the consequences of different mass-loss histories on post-AGB time scales we have also calculated the post-AGB evolution of the sequence with ($M_{\rm ZAMS}$, $M_{\rm H}$)=($3M_\odot, 0.836M_\odot$). Please note that this combination of initial and final mass does not agree with empirical relationships (see Fig. 1). Figure 10 illustrates the evolution of the two models with equal remnant mass ($0.836M_\odot$) but different different initial masses (3 and $5M_\odot$) in comparison with the ($M_{\rm ZAMS}$, $M_{\rm H}$)=($3M_\odot, 0.605M_\odot$) sequence, whereas Fig. 11 shows the corresponding picture for the evolution of $L_{\rm g}$, L_ν and $L_{\rm sur}$ as a function of time. The time scales of the two $0.834M_\odot$ remnants are quite different: The model based on

[1] Tables 3 and 4 are only available in electronic form at the CDS via anonymous ftp 130.79.128.5.

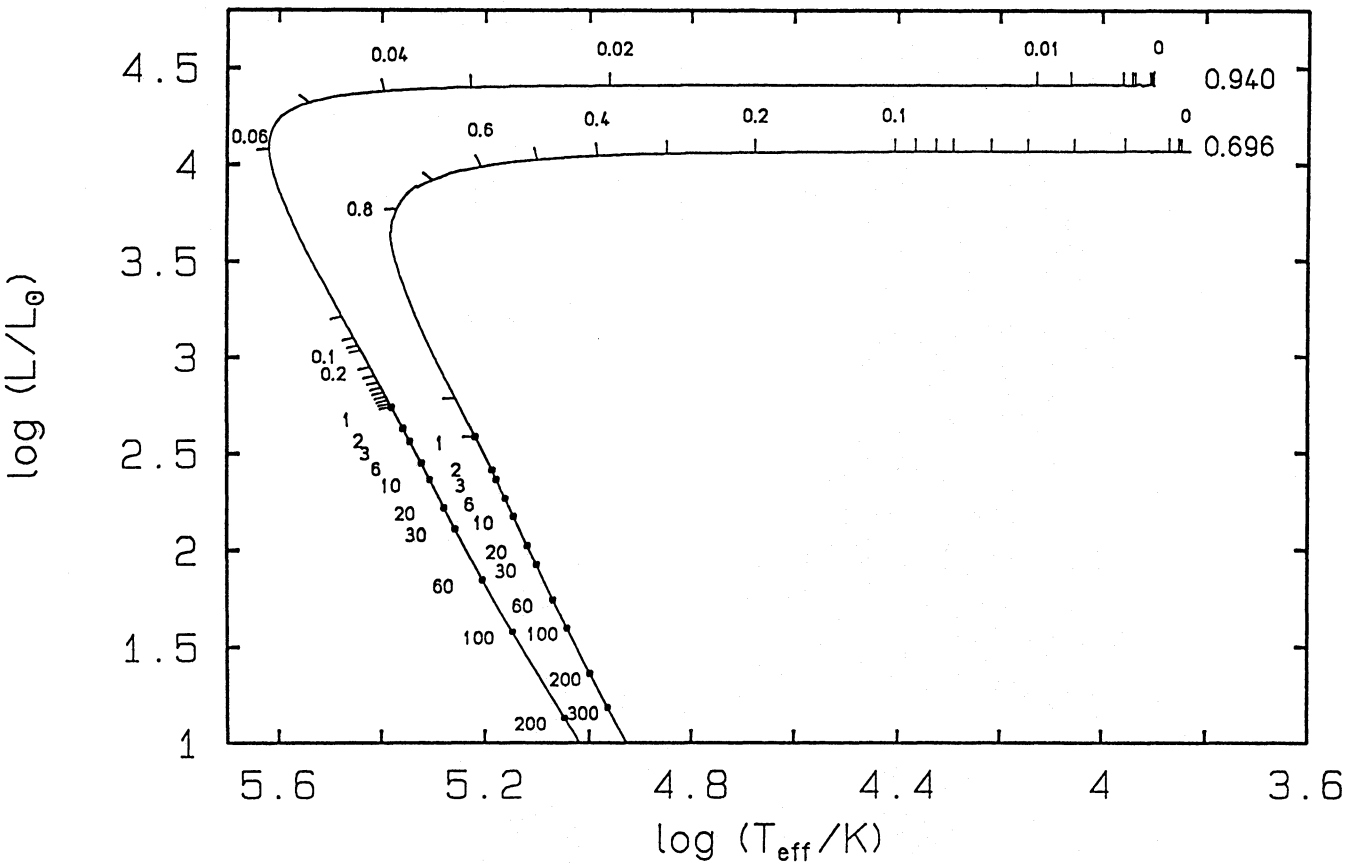

Fig. 8. Evolution of post-AGB models with $(M_{\rm ZAMS}, M_{\rm H}) = (4M_\odot, 0.696M_\odot)$ and $(7M_\odot, 0.940M_\odot)$. Time marks are in units of 10^3 yrs

a $3M_\odot$ progenitor needs only $\approx$ 150 yrs instead of 420 yrs for the horizontal part of the evolution due to its smaller envelope mass at the tip of the AGB. Concerning the fading part we get now time scales similar to those of Wood & Faulkner (1986). The rapid luminosity drop after the exhaustion of nuclear shell burning is larger than for the model with $(5M_\odot, 0.836M_\odot)$ reflecting the $L_{\rm g}$ difference at the tip of the AGB. For example, at $t = 10^3$ yrs the surface luminosity is approximately only half as large as the one of the consistent remnant. The following evolution is determined by the thermomechanical structure of the models. The $(3M_\odot, 0.836M_\odot)$ remnant is the most compact and degenerate object due to its very long AGB evolution, and fades fastest. On the other hand, the structure of the $(5M_\odot, 0.836M_\odot)$ remnant is less compact at significantly higher internal temperatures This model fades even slower than the $0.605M_\odot$ remnant. Looking at Fig. 11 one sees that the different fading is mainly due to the different temporal evolution of $L_{\rm g}$. In the case of the $(3M_\odot, 0.836M_\odot)$ remnant the decrease of $L_{\rm g}$ is much steeper than for the other massive model. For instance, at $t = 10^4$yrs $L_{\rm g}$ has decreased by a factor of 4.4 instead of 2. At $3 \cdot 10^5$yrs the gravothermal luminosity of the $(5M_\odot, 0.836M_\odot)$ model falls below the one of the $0.605M_\odot$ remnant. Finally, at $t \approx 2 \cdot 10^7$yrs, roughly coinciding with the point where neutrino losses do not accelerate the evolution any longer, both massive remnants have the same the gravothermal luminosity and are fading slower than the less massive one. Correspondingly, at low surface luminosities ($< 0.1L_\odot$) the timescales of both massive remnants become equal because their thermomechanical structure has become almost equal in the meantime. Only now the evolution of the models does not depend on their history any longer.

This different fading behaviour can be explained in terms of energy changes. Consider a gravitationally bound system with the total energy $W = E_{\rm ion} + E_{\rm el} + \Omega$ ($E_{\rm ion}$, $E_{\rm el}$: internal energy of the ions and the electrons, resp.; Ω: gravitational energy). For simplicity we neglect Coulomb energies and do not consider crystallization which both do not change the following estimation. By means of the virial theorem

$$\zeta(E_{\rm ion} + E_{\rm el}) + \Omega = 0, \tag{7}$$

with $1 \le \zeta \le 2$ depending on the equation of state, it can be easily shown (cf. Cox & Giuli 1968; Kippenhahn & Weigert 1990) that the luminosity L of the system is given by

$$L = -\dot{W} = (\zeta - 1)(\dot{E}_{\rm ion} + \dot{E}_{\rm el}) \tag{8}$$

The loss of total energy by radiation ($L > 0$) requires contraction ($\dot{\Omega} < 0$) and an increase of the total internal energy $\dot{E}_{\rm ion} + \dot{E}_{\rm el} > 0$. In the case of an ideal and non-degenerate gas ($\zeta = 2$) we have equipartition with $E_{\rm ion} \sim E_{\rm el} \sim T$ which

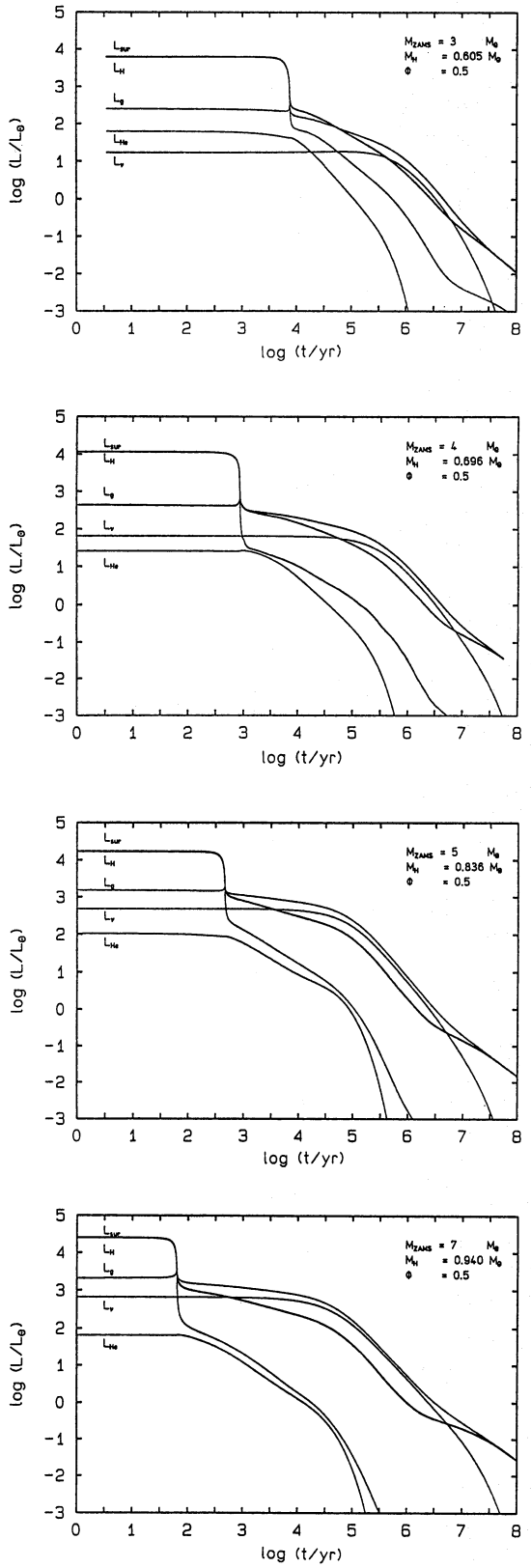

Fig. 9. Surface luminosity ($L_{\rm sur}$) and luminosity contributions due to hydrogen ($L_{\rm H}$) and helium ($L_{\rm He}$) burning, gravothermal energy releases ($L_{\rm g}$) and neutrino losses (L_ν) as a function of time for the sequences shown in Figs. 7 and 8

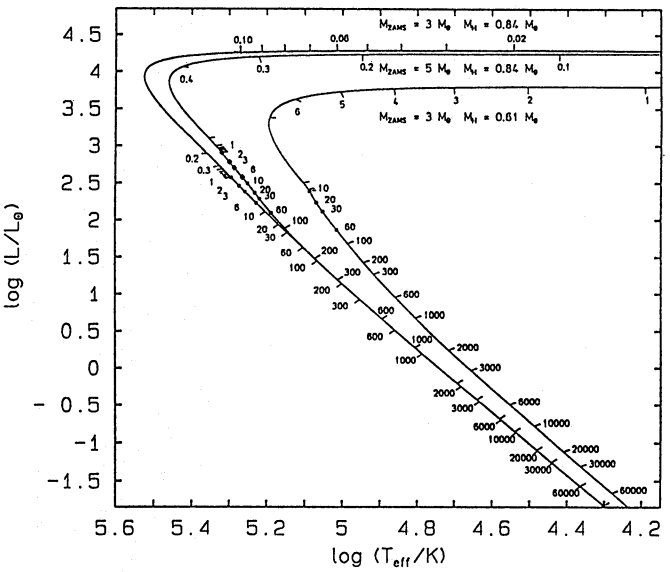

Fig. 10. Evolution of post-AGB models with $(M_{\rm ZAMS}, M_{\rm H}) = (3M_\odot, 0.61M_\odot), (5M_\odot, 0.84M_\odot)$ and $(3M_\odot, 0.84M_\odot)$. Time marks are in units of 10^3 yrs ($\phi = 0.5$)

leads to a heating of the system ($\dot{T} > 0$). However, considering a star in which the electrons are degenerate one has to distinguish between ion and electrons because a certain amount of the gravitational energy change $\Delta\Omega$ is used up to increase the Fermi energy of the electrons. For strongly degenerate systems, it even follows that $\Delta\Omega$ and $\Delta E_{\rm el}$ almost compensate each other, and the energy balance $L = -\dot{E}_{\rm ion} - \dot{E}_{\rm el} - \dot{\Omega}$ gives $L = -\dot{E}_{\rm ion} \sim -\dot{T}$. Thus the loss of energy by radiation is nearly equal to the release of ionic thermal energy, and the star cools. However, this equivalence should not be interpreted as if the luminosity of a white dwarf is only provided by the expense of thermal energy and compression terms are without meaning. Due to the virial theorem the gravitational changes are leading to a continuous increase of the white dwarf's total internal energy. For a discussion of the virial theorem and energy contents of white dwarfs see also Koester (1978) and Koester & Chanmugam (1990).

In terms of the star's response to radiative energy losses the evolution from the main sequence to the stage of white dwarfs can be roughly described as follows (for $M > 2M_\odot$): On the main sequence the models are non degenerate and contraction is connected with heating. After the exhaustion of central helium-burning the core begins to degenerate. The degeneracy increases during the AGB evolution and a fraction of the energy released by contraction is used up by raising the Fermi energy of the electrons, being no longer available for the increase of the thermal energy. However, $L_{\rm g}$ is still dominated by the ideal and weakly degenerate layers of the outer core and the contraction leads to a heating of the interior (finally, neutrino losses cause a cooling of the interior). After the model has left the AGB the strongly degenerate layers become more and more important. At the latest these layers determine the response to energy losses by radiation when nuclear shell burning ceases and the surface luminosity drops rapidly. Then, contraction is connected with

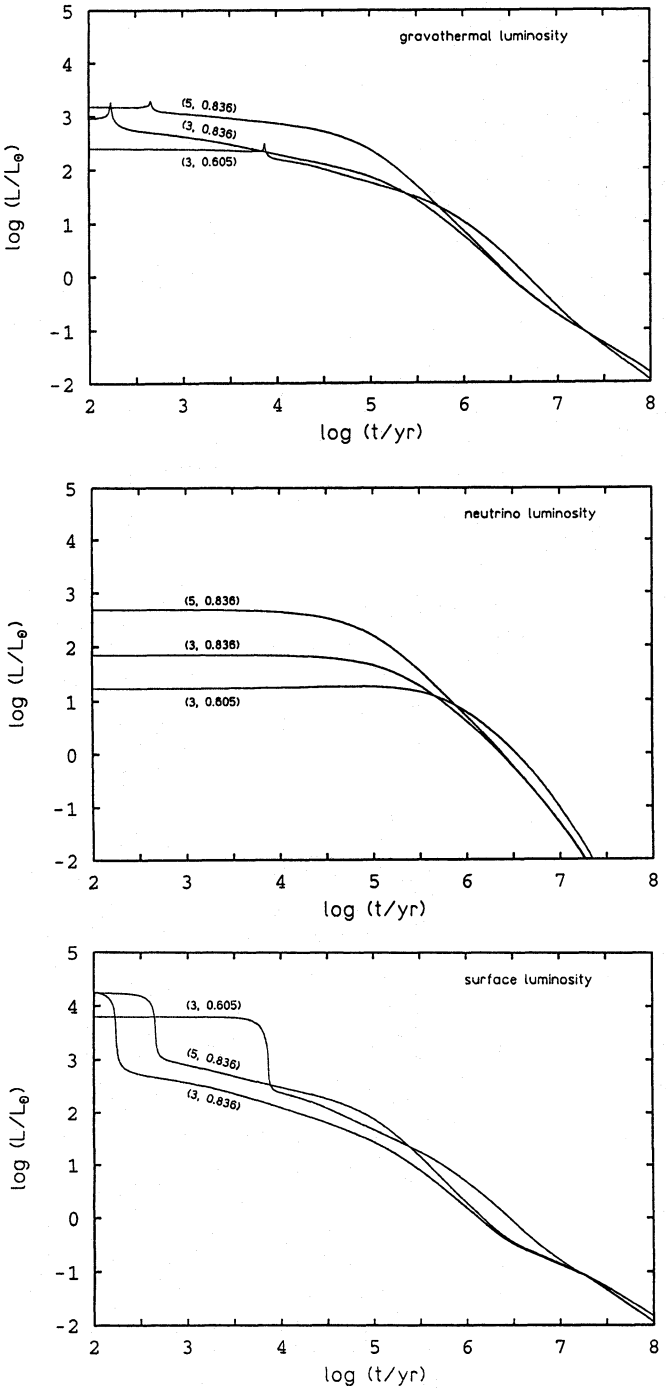

Fig. 11. Gravothermal luminosity, neutrino losses and surface luminosity of post-AGB models with $(M_{\rm ZAMS}, M_{\rm H}) = (3M_\odot, 0.61M_\odot)$, $(5M_\odot, 0.84M_\odot)$ and $(3M_\odot, 0.84M_\odot)$ as a function of time

cooling, the energy radiated away becomes equal to the decrease of ionic thermal energy since almost the whole energy liberated by contraction is compensated by the increase of the electronic Fermi energy.

Thus, the more degenerate a model leaves the AGB, i.e. the more compact and cooler the interior, the faster is the fading. Since for a given initial mass the mean degeneracy increases with increasing AGB duration, i.e. final mass, it is no suprise that the models of Paczynski (1971) and of Wood & Faulkner (1986) fade faster with increasing core mass because they are based on a single initial mass. The same holds for our two remnants of 0.605 and $0.836M_\odot$ belonging to the $3M_\odot$ progenitor. On the other hand, for a given final mass the models belonging to larger initial masses fade slower since they are hotter and less compact. This explains the different fading times in the case of both $0.836M_\odot$ remnants.

The fading time scales of the remnants with $(M_{\rm ZAMS}, M_{\rm H})$=$(4M_\odot, 0.696M_\odot)$ and $(7M_\odot, 0.940M_\odot)$ confirm again the conclusion that more massive remnants can fade much more slowly than hitherto assumed. Looking at the most massive remnant of $0.94M_\odot$ one sees that $\log(L/L_\odot) = 2.1$ is reached within 30000 yrs whereas the $0.696M_\odot$ remnant needs only 14000 yrs.

Comparing the 0.940 remnant with the slow $0.836M_\odot$ model it turns out that the $0.940M_\odot$ model does not fade slower although both remants are consistent with the initial-final mass relation. However, taking into account that only models with the same or at least with a similar mass-loss history should be compared explains this apparent contradiction.

As discussed above the fading times decrease with increasing final mass for a given initial mass. In the case of $M_{\rm ZAMS} = 7M_\odot$ we have calculated two mass-loss histories: One sequence with $\dot{M}_{\rm B1}$ (15 thermal pulses, $M_{\rm final} = 0.923M_\odot$) and one with $\dot{M}_{\rm BH}$ and an artifically invoked superwind (31 thermal pulses, $M_{\rm final} = 0.940M_\odot$). The difference of the final masses are only small due to the small core growth rate for larger initial masses, and both remnants are consistent with the initial-final relation although their lifetimes on the TP-AGB differs by a factor of 2.3 (see Blöcker 1994).

The $0.923M_\odot$ model begins the post-AGB evolution as a helium burner with $\phi \approx 0$. Since our treatment of mass loss (e.g. $\dot{M}_{\rm B1}$ on the AGB and $\dot{M}_{\rm trans}$ in the immediate vicinity of the AGB) provides in most cases hydrogen burning models (with $\phi \approx 0.5$) the timescales of the $0.924M_\odot$ model would not be comparable, and we have not followed the central-star evolution. Instead, we have calculated the post-AGB evolution of the $0.940M_\odot$ remnant in order to get corresponding time scales for a very massive hydrogen burning model.

Due to the longer AGB evolution the $0.940M_\odot$ model is cooler and more contracted in its interior than the $0.923M_\odot$ remnant (Fig. 2). Furthermore the gravothermal luminosity at the tip of the AGB is much smaller (Fig. 3). Both leads to a faster fading. It can easily be estimated that a hydrogen-burning $0.923M_\odot$ remnant (e.g. a model which has suffered from a Bowen-like mass loss) will indeed fade slower than the model with $(5M_\odot, 0.836M_\odot)$, at least in the upper part of the fading

regime. Thus, it seems to be quite safe to state that the fading speed of more massive models decreases with increasing remnant mass if a mass-loss law like $\dot{M}_{\rm B1}$ is applied on the AGB.

The sensitivity of the fading time scales with respect to the AGB history becomes also apparent by the comparison with the results of Vassiliadis & Wood (1994). Their models cover remnant masses of 0.569 to $0.9M_\odot$ and fade contrary to our models always the faster, the higher the core masses. Whereas the time scales for core masses of about $0.6M_\odot$ are quite similar to ours they deviate appreciably for more massive remnants. For instance, the $0.9M_\odot$ remnant (with $M_{\rm ZAMS} = 5M_\odot$) of Vassiliadis & Wood (1994) reaches $\log(L/L_\odot) = 2.1$ in only $\approx$ 6400 yrs! Since the only difference of these two sets of post-AGB calculations is the treatment of mass-loss (Vassiliadis & Wood (1994) assume lower rates), which is not important for the cooling part of the evolution, it is obvious that, again, the conflict of the evolutionary rates must be due to the respective AGB models on which the calculations are based (i.e. Vassiliadis & Wood 1993; Blöcker 1994). Vassiliadis & Wood (1993) employed lower mass-loss rates along the AGB than we did (cf. Fig.1). Thus, for a given initial mass their remnants are older and more degenerate. As discussed above this leads to a faster fading.

Finally, we want to give some interpretation of observational data. For this purpose we take now only models into account which are consistent with the empirical initial-final mass relation of Weidemann (1987). Figure 12 shows the corresponding evolutionary tracks complemented with the low-mass models of Schönberner (1983). The given isochrones indicate that the least luminous central stars of planetary nebulae should have masses of $\approx 0.65M_\odot$ (Blöcker & Schönberner 1990).

In order to study the fading part of the central-star evolution in comparison with observations we follow the discussion of Schönberner (1993): Many planetary nebulae of hot and faint central stars appear optically thick in the Lyman continuum. On the other hand, models of planetary nebulae along tracks for hydrogen-burning central stars indicate that the fast luminosity drop after the exhaustion of nuclear shell burning leads to optically thick nebulae (Schmidt-Voigt & Köppen 1987; Schönberner & Tylenda 1990; Marten & Schönberner 1991) with ionized masses of a few $1/10M_\odot$. Consequently, for such objects the Zanstra method is applicable for the temperature determination, and even the Shklovsky method can be used for the determination of distances.

The observational data shown in Fig. 12 has been taken from Jacoby & Kaler (1989) and Kaler & Jacoby (1989). From 82 listed galactic planetary nebulae we have selected those objects (29) which are optically thick and whose loci in the HR diagram can be determined by Zanstra temperatures ($T_{\rm HI} \approx T_{\rm HeII}$) and Shklovsky distances ($M_{\rm ion} = 0.2M_\odot$).

Most of the objects are found in the regions where the fading speed of our models decreases considerably. For example, all very hot and presumably more massive central stars of this sample ($M \gtrsim 0.8M_\odot$) are located well above $\log(L/L_\odot) = 2$, some even above $\log(L/L_\odot) = 2.5$.

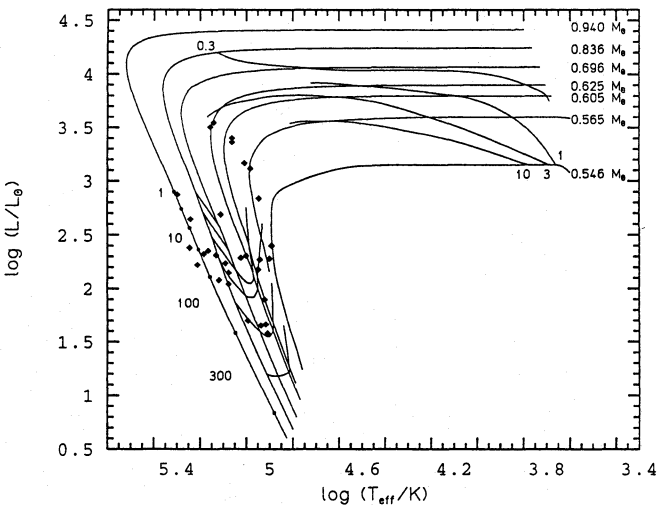

Fig. 12. Isochrones for several evolutionary tracks with observational data. Time marks are in units of 10^3yrs

As outlined by Schönberner (1993) the distances to these hot and low-luminous central stars may have been been underestimated since the accretion of matter from the old AGB wind (cf. Marten & Schönberner 1991) increases the ionized nebular mass. However, increasing the distances to these old objects would correspond to an upward vertical shift of their loci in Fig. 12 leading to even higher luminosities.

For an post-AGB age of $t = 10^4$ yr Fig. 13 shows the luminosity as a function of the core mass ($\approx$ remnant mass) for the models presented here as well as for those of Vassiliadis & Wood (1994). It can be clearly seen that the models of Vassiliadis & Wood are up to $\approx$ 0.4 dex less luminous than our ones for more massive remnants at this particular age. Correspondingly, an accumulation of objects can be expected for $\log(L/L_\odot) \approx 2.1...1.9$ instead for $\log(L/L_\odot) \approx 2.5...2.3$. For $t = 3 \cdot 10^3$ and $3 \cdot 10^4$ yr we get for the 0.836 and $0.94M_\odot$ remnants luminosity intervalls of $\log(L/L_\odot) = 2.56...2.71$ and 2.29...2.11, resp. At the same post-AGB ages the luminosity of the $0.9M_\odot$ remnant of Vassiliadis & Wood (1994) amounts to $\log(L/L_\odot) = 2.3$ and 1.64.

The position of the corresponding helium burning models is also shown in Fig. 13. Whereas they evolve much slower than hydrogen burning models for low-mass stars the situation gets again complex for massive remnants. In our example for $t = 10^4$ yr it is hard to distinguish between the He burning and the slowly fading H burning model for $M_{\rm H} = 0.836M_\odot$. Both have nearly the same luminosity.

Therefore, in the Vassiliadis & Wood (1994) scenario massive and luminous central stars are most likely helium burning objects whereas our results suggest that they can equally well explained by hydrogen burning remnants.

5.2. Helium burning models

According to Iben (1984) the post-AGB evolution is dominated by helium burning if the star leaves the AGB with a thermal-

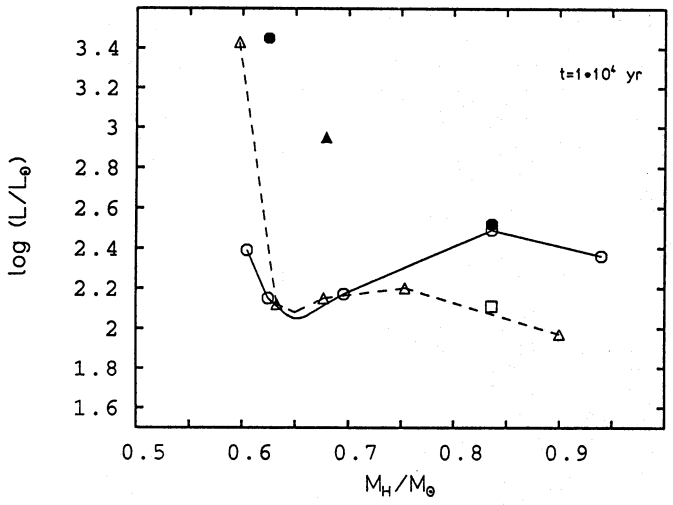

Fig. 13. Luminosity vs. core mass at $t = 10^4$ yr for hydrogen burning (open symbols) and helium burning models (filled symbols). The triangles correspond to the results of Vassiliadis & Wood (1994) (the helium burner refer to Z=0.008, all other models to Z=0.016), the circles to the models presented here. The square denote the position of the $0.836M_\odot$ remnant belonging to $M_{\rm ZAMS} = 3M_\odot$ instead to $5M_\odot$

pulse cycle-phase of $0 \leq \phi \leq 0.15$. This has been the case for our $0.923M_\odot$ model for which, however, we have not calculated the post-AGB evolution. For $0.15 \leq \phi \leq 0.3$ both nuclear shell sources contribute equal luminosity fractions, for $0.3 \leq \phi \leq 1.0$ hydrogen burning determines the nuclear energy production ($L_{\rm He} \approx 0.1 L_{\rm H}$).

If the thermal-pulse cycle-phase is sufficiently large. i.e. close to 1, a last thermal pulse can occur during the post-AGB evolution transforming a hydrogen burning into a helium burning model. Then, the model quickly evolves back to the AGB, starting there the post-AGB evolution again as a helium burner (cf. Iben 1984; see Figs. 14 - 16 and Table 5)[2]. Typically $\phi \gtrsim 0.9$ is required for such a late pulse.

Besides of the standard mass-loss reduction between 100 and 50 d we additionally calculated a sequence for the $0.625M_\odot$ remnant conducting the reduction earlier, namely between 150 and 100 d. Since the mass-loss rates are decreasing relatively close to the AGB the reduction time increases from 778 to 2845 yrs leading to a larger thermal-pulse cycle phase at the respective beginning of the post-AGB evolution. Now, ϕ is sufficiently large for a thermal pulse to occur. Figure 14 shows the corresponding evolution in the HR diagram. Please note that $t = 0$ refers here to $P_0 = 100$ d instead to $P_0 = 50\,d$ which is reached at $t = 6000$ yrs.

Along the horizontal part the model evolves like the "normal" hydrogen burners but immediate before the exhaustion of nuclear shell burning the helium shell becomes thermally unstable. The surface luminosity drops more than one order of magnitude in only 10 yrs and the model evolves quickly back to the AGB in $\approx$ 200 yrs. After reaching a luminosity maximum the model starts again the post-AGB evolution. Because it is now a helium burner the evolutionary speed is considerably lower ($\approx$ factor 3). Due to the continuous mass loss during this relatively slow evolution the envelope mass is reduced to such an extent that the hydrogen burning shell reignites only mildly and the helium burning shell continues to provide the major part of nuclear energy. Thus, an increase of the surface luminosity due to a "complete" ignition of the hydrogen burning shell is missing (see Fig. 16 for the shape of such a luminosity increase) and the model begins to fade.

Additionally, we have also calculated the corresponding evolution for a more massive model. For that purpose we split the $(M_{\rm ZAMS}, M_{\rm H}) = (5M_\odot, 0.836M_\odot)$ sequence and temporarily diminished the mass-loss rates at the tip of the AGB in such a way that the thermal-pulse cycle-phase increases sufficiently. The corresponding track is shown in Fig. 15. Due its larger core mass this model needs only $\approx$ 50 yrs for its evolution back to the AGB,

Such evolutionary tracks can be used to model the evolution of Fg Sge (cf. Iben 1984) which is supposed to have suffered from a late helium flash. By means of the evolution of the bolometric magnitude which depends strongly on the core mass estimates for the mass of Fg Sge can be given (Blöcker & Schönberner 1994).

Finally, we want to report on the evolution of the model with $M_{\rm ZAMS} = 1M_\odot$ whose AGB evolution was terminated at $M_{\rm H} = 0.524M_\odot$ even before the first thermal pulse was reached. This model lost 30% of its initial mass already on the RGB and it left the AGB before a period of 100 d was reached. Thus, a transition from $\dot{M}_{\rm R}$ to $\dot{M}_{\rm B1}$ did not take place and the maximum mass-loss rate at the tip of the AGB amounted only to $\approx 10^{-7} M_\odot$/yr. The first thermal pulse occured during the post-(E)AGB evolution. Due to the very slow evolution of low-mass post-AGB stars the model suffers even from a *second* thermal pulse. Figure 16 shows the corresponding evolutionary track and Fig. 17 the temporal evolution of the different luminosity contributions. Age zero refers to $P_0 = 50$ d.

At $t = 8400$ yrs the helium shell gets thermally unstable leading to a luminosity drop of ≈ 0.4 dex within 400 yrs which is followed by a evolution back to the vicinity of the AGB in $\approx$ 1000 yrs. The post-AGB evolution starts again and 3000 yrs later the hydrogen reignites leading to a increase of the surface luminosity (and to a "hook" in the track). Since the very first thermal-pulse periods are always small (in the third part of this series we will give a detailed overview of thermal-pulse properties) and the evolutionary speed of the model is low due to its small mass (and due to the helium burning phase), a second thermal pulse takes place at $t \approx 86000$ yrs. Because this instability is much more stronger than the first one ($L_{\rm He}^{\rm max} = 6.25 \cdot 10^4 L_\odot$ instead of $1.38 \cdot 10^4 L_\odot$) the corresponding loop in the HR diagram is more pronounced. This instability is followed by a small subpulse at $t = 90000$ yrs corresponding to additional loop which, however, is only small. Finally the hydrogen burning shell reignites the second time and the surface luminosity increases considerably again. After almost 150000 yrs the horizontal evolution is finished and the model begins to fade.

[2] Table 5 is only available in electronic form at the CDS via anonymous ftp 130.79.128.5.

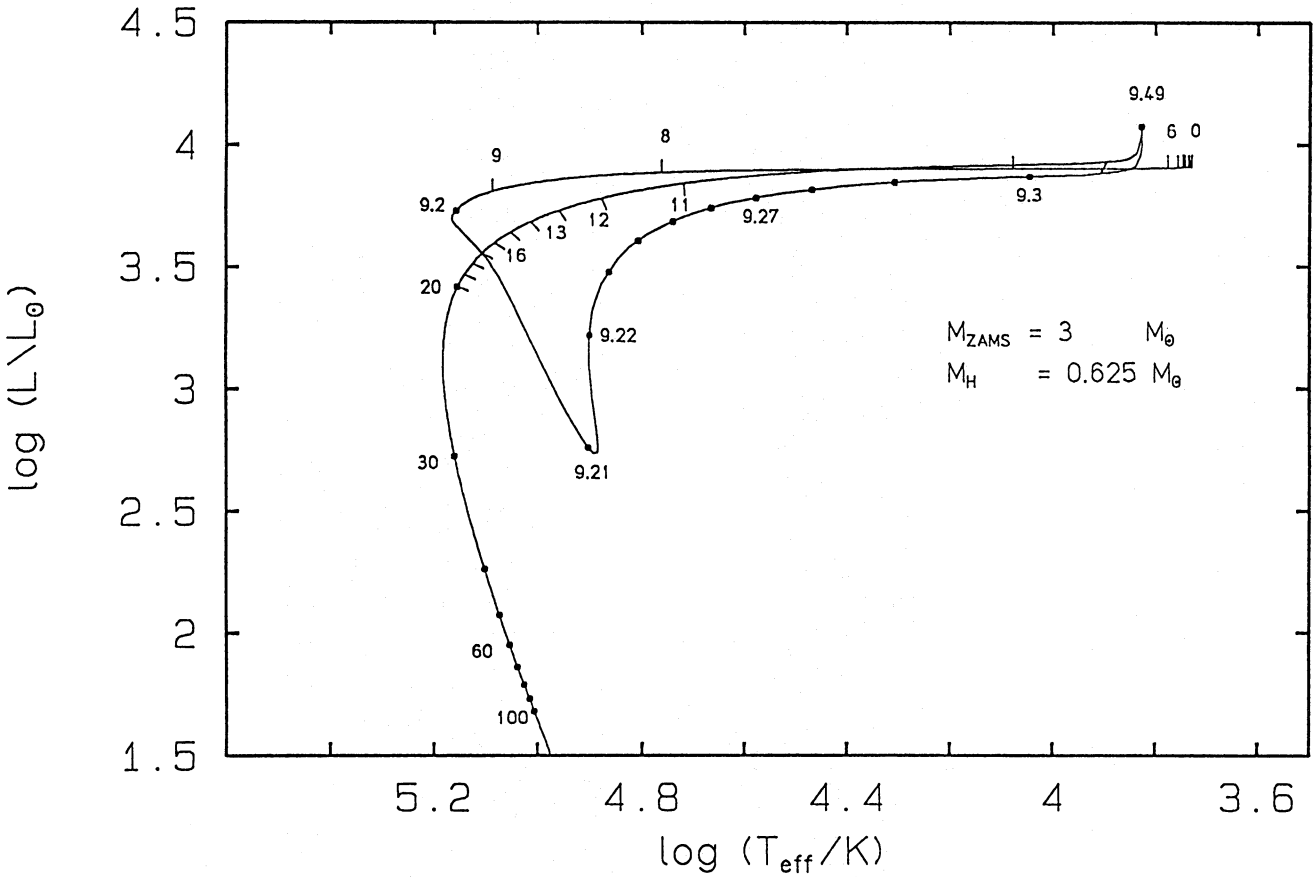

Fig. 14. Evolution of a post-AGB models with $(M_{\rm ZAMS}, M_{\rm H}) = (3M_\odot, 0.625M_\odot)$. Time marks are in units of 10^3 yrs ($\phi = 0.87$)

Two thermal pulses during the post-AGB evolution are only likely for models of low evolutionary speed and sufficiently small thermal-pulse periods, e.g. for models with $M_{\rm ZAMS} \lesssim 3M_\odot$ and $M_{\rm H} \lesssim 0.55M_\odot$ which have only suffered from a few thermal pulses, or even from none, on the AGB. Furthermore, the thermal-pulse phase ϕ at the beginning of the post-AGB evolution should be sufficiently large (> 0.8). Dorman et al. (1993) calculated the post-EAGB evolution for models of different metallicities. Some of their models are also suffering from a second thermal pulse. Small mass-loss rates at the tip of the AGB (e.g. $10^{-7}M_\odot$/yr) yield very large transition times to the central-star region increasing the thermal-pulse phase appreciably. Thus, the lack of a superwind makes multiple post-AGB helium flashes more likely.

On the other hand, as discussed by Vassiliadis & Wood (1994), the interflash times of high-mass models, e.g. of $0.9M_\odot$, amount to typically several thousand years leading to the possibility of repeated shell flashes if the transition time is sufficiently longer (at least a factor of 2). However, this requires an early mass-loss stop at rather low effective temperatures.

6. Conclusions

Already at the tip of the AGB it becomes obvious that the mass-loss history plays an important role for the time scales of central-stars of planetary nebulae, and that in the case of different histories the fading time scales can be expected to be different, too.

The longer the evolution on the AGB, the more degenerate is the interior of a star, and thus the faster is the fading due to the larger fraction of potential energy which is used up to raise the Fermi energy of the electrons, being no longer available for the thermal content of the star. Since the models of Paczyński (1970) and Wood & Faulkner (1986) are based on only *one* initial mass their fading times had to decrease with the models' core masses like in the case of our 0.605 and $0.836M_\odot$ remnants with $M_{\rm ZAMS} = 3M_\odot$.

On the other hand, we have shown that models which are consistent with reliable initial-final mass relationships may fade *slower* the larger their core masses. Hence, to agree with observed initial-final mass relations is essential for the consideration of fading time scales.

However, the situation remains somewhat uncertain in the case of more massive remnants correctly belonging to high-mass progenitors. For instance, although both remnants of 0.940 and $0.923M_\odot$ are consistent with the initial-final mass relation their fading time scales are somewhat different. The $0.940M_\odot$ remnant fades slower than the one with $0.696M_\odot$ but faster than the one with $0.836M_\odot$, whereas the slightly lighter $0.923M_\odot$ remnant will also fade slower than the $0.836M_\odot$ model due to its

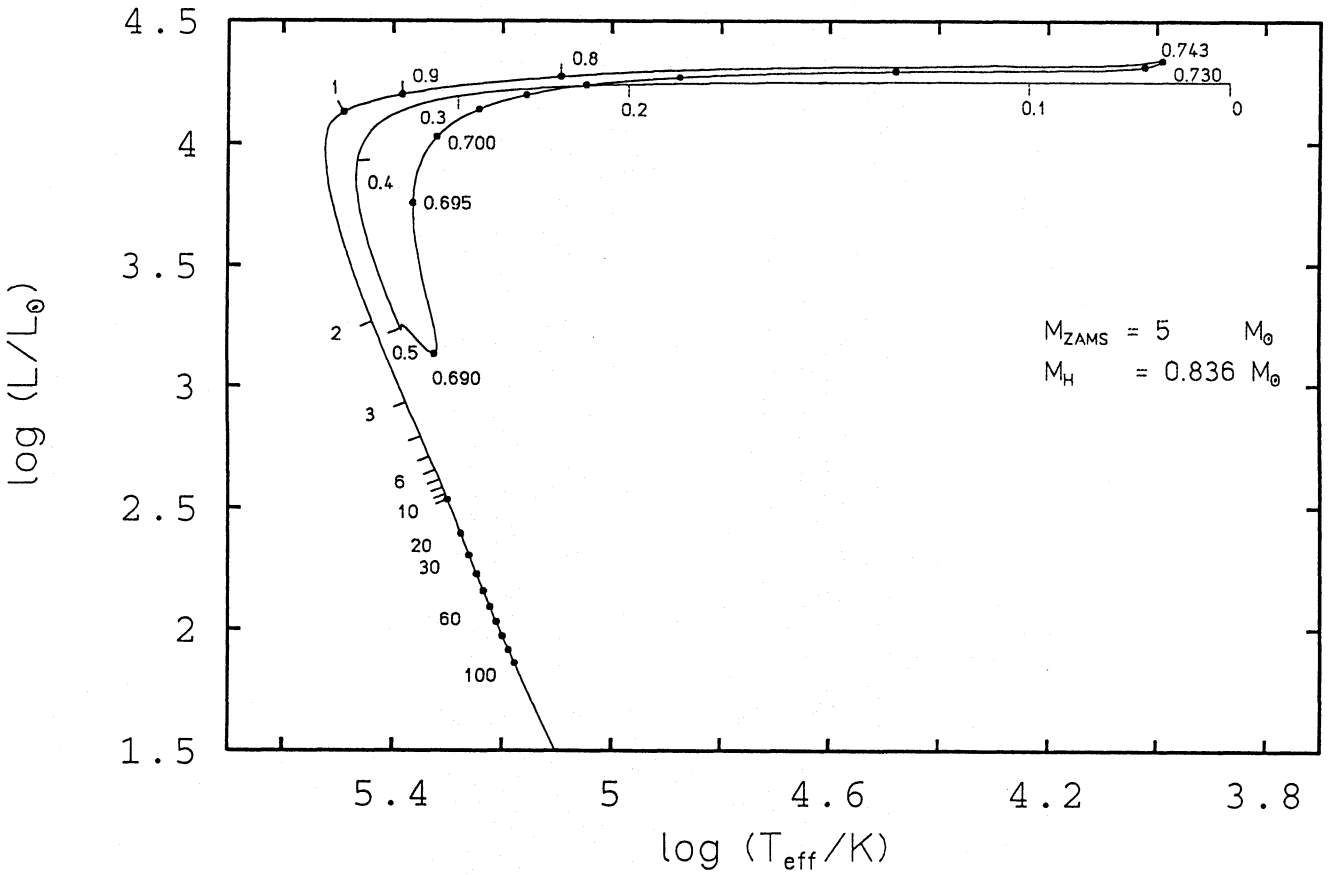

Fig. 15. Evolution of a post-AGB models with $(M_{\rm ZAMS}, M_{\rm H}) = (5M_{\odot}, 0.836M_{\odot})$. Time marks are in units of 10^3 yrs ($\phi = 0.9$)

shorter AGB evolution. The core growth rate per thermal pulse of such massive remnants is only small (e.g. $\approx 10^{-3}M_{\odot}$) and different mass-loss laws allowing different number of thermal pulses to occur (e.g. 15 and 31, resp.) lead to only slightly different final masses. However, the thermomechanical structures can differ considerably.

Taking now only models into account which have suffered from a strongly accelerated mass-loss on the AGB, as described, for example, by our mass-loss law $\dot{M}_{\rm B1}$ derived from the results of Bowen (1988), and which are consistent with the empirical initial-final mass relation of Weidemann (1987), it indeed turns out that more massive remnants seem to fade generally slower than less massive ones. Consequently, the least luminous central stars are not necessarilly the most massive ones but may instead belong to masses of $\approx 0.65M_{\odot}$ (cf. Blöcker & Schönberner 1990).

The fact that the fading time scales depend sensitively on the AGB mass-loss history in the way discussed above explains why the more massive models of Vassiliadis & Wood (1994) fade faster than their lighter ones conflicting with our results. For given initial masses their models have spent a longer time on the AGB leading to higher remnant masses (cf. Fig. 1) and a stronger mean degeneracy of the cores.

Finally, also the mass-loss rates beyond the AGB are crucial parameters for evolutionary time scales. Particularly, they determine the transition time from the AGB to the central-star region (Schönberner 1989). In which temperature range and how the high AGB mass-loss drops by order of magnitudes is up to now only poorly known. We have considered a non-abrupt decrease of the AGB rates as suggested by dust-shell calculations (cf. Bedijn 1987) and coupled the reduction to the decreasing pulsational period. The corresponding transition times are shorter than those of Vassiliadis & Wood (1994) since they stopped mass-loss earlier. Our treatment of mass-loss leads preferably to hydrogen burning models.

Hydrodynamical pulsation calculations of Zalewski (1994) indicate that at least for low-mass post-AGB models (e.g. $0.6M_{\odot}$) mass-loss should "stop" somewhere between $\log T_{\rm eff} \approx 3.8...3.9$ which nicely coincides with the end of our mass-loss reduction at $P_0 = 50$ d. Work is in progress to study the strong decrease of mass-loss in more detail.

Acknowledgements. I am grateful to Prof. D. Schönberner for many discussions and valuable suggestions. Thanks go also to Dr. J. Zalewski for providing us with the data of his pulsational calculations. I would also like to thank the referee for instructive remarks. Funding by the Deutsche Forschungsgemeinschaft (Scho 394/1-1) is acknowledged. Most of the calculations presented here have been performed at the

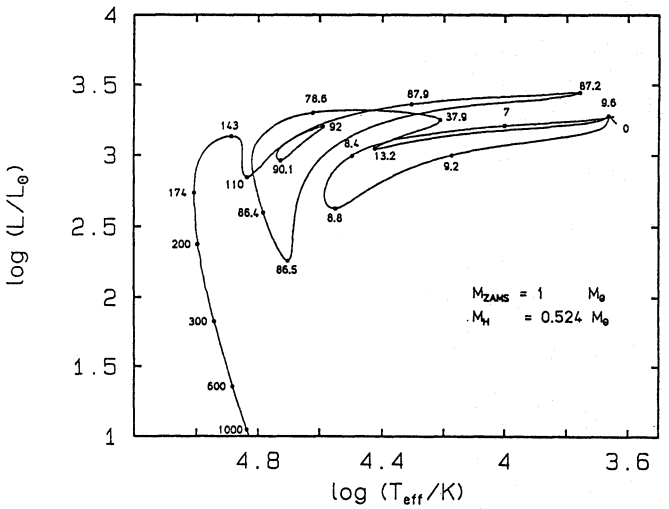

Fig. 16. Evolution of a post-AGB models with $((M_{\rm ZAMS}, M_{\rm H}) = (1M_\odot, 0.524M_\odot)$ with two thermal pulses. Time marks are in units of 10^3 yrs

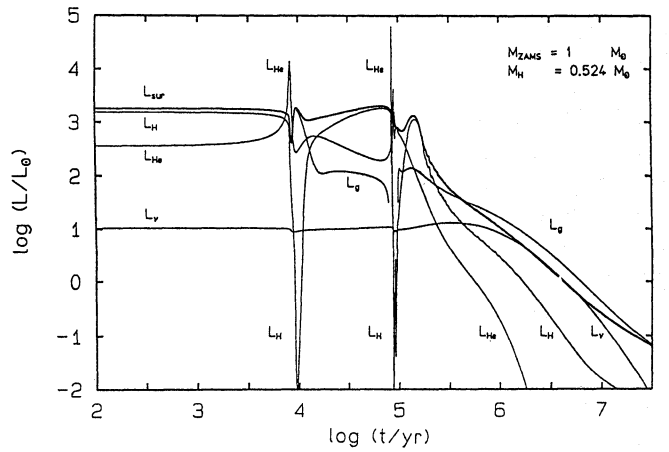

Fig. 17. Surface luminosity ($L_{\rm sur}$) and luminosity contributions due to hydrogen ($L_{\rm H}$) and helium ($L_{\rm He}$) burning, gravothermal energy releases ($L_{\rm g}$) and neutrino losses (L_ν) as a function of time for the sequence with $((M_{\rm ZAMS}, M_{\rm H}) = (1M_\odot, 0.524M_\odot)$

Institut für Astronomie und Astrophysik in Kiel. The computations were conducted on the CRAY-XMP and -YMP of the Rechenzentrum der Universität Kiel.

References

Baud, B., Habing, H.J.: 1983, A&A 127, 73
Bedijn, P.J., 1987, A&A 186, 136
Blöcker, T.: 1989, Diploma thesis, University of Kiel
Blöcker, T.: 1993a, PhD thesis, University of Kiel
Blöcker, T.: 1993b, in *White Dwarfs: Advances in Observation and Theory*, ed. M.A. Barstow, NATO ASI Series C, Kluwer, Dordrecht, p. 59
Blöcker, T.: 1993c, Acta Astron. 43, 305
Blöcker, T.: 1994, A&A, in press
Blöcker, T., Schönberner, D., 1990, A&A 240, L11
Blöcker, T., Schönberner, D., 1994, in preparation
Bowen, G.H., 1988, ApJ 329, 299
Cox, J.P, Giuli, R.T., 1968, Principles of Stellar Structure, Vol. 1&2, Gordon and Breach, New York
Cox, A.N., Stewart, J.N., 1970, ApJS 19, 243
Dorman, B., Rood, R.T., O'Connell, R.W., 1993, ApJ 419, 596
Habing, H.J., te Lintel Hekkert, P., van der Veen, W.E.C.J., 1989, in *Planetary Nebulae*, IAU Symp. 131, ed. S. Torres-Peimbert, Kluwer, p. 359
Iben, I. Jr., 1984, ApJ 277, 333
Jacoby, G.H., Kaler, J.B., 1989, AJ 98, 1662
Kaler, J.B., Jacoby, G.H., 1989, ApJ 345, 871
Kippenhahn, R., Weigert, A., 1990, Stellar Structure and Evolution, Springer, Berlin
Koester, D., 1978, A&A 64, 289
Koester, D., Chanmugam, G. 1990, Rep. Prog. Phys. 53, 857
Likkel, L., Omont, A., Morris, M., Forveille, T., 1987, A&A 173, L11
Luck, R.E., Bond, H.E., 1984, ApJ 279, 729
Maeder, A., Meynet, G., 1989, A&A 210, 155
Marten, H., Schönberner, D., 1991, A&A 248, 590
Ostlie, D., Cox, A.N.: 1986, ApJ 311, 864
Paczyński, B., 1970, Acta Astron. 20, 47
Paczyński, B., 1971, Acta Astron. 21, 417
Parthasarathy, M., 1993, in *Luminous High Lattitude Stars*, ed. D. Sasselov, ASP Conference Series, Vol. 45, p. 173
Parthasarathy, M., Pottasch, S.R., 1986, A&A 154, L16
Pauldrach, A.; Puls, J., Kudritzki, R.P., Méndez, R., Heap, S.R.: 1988, A&A 207, 123
Perinotto, M.: 1989, IAU Symp. No 131 *Planetary Nebulae*, ed. S. Torres-Peimbert, Reidel, Dordrecht, p. 293
Pottasch, S.R., Partharasathy, M., 1988, A&A 192, 182
Reimers, D., 1975, "Problems in Stellar Atmospheres and Envelopes", B. Baschek, W.H. Kegel, G. Traving (eds.), Springer, Berlin, p. 229
Renzini, A., 1981, in *Physical Processes in Red Giants*, eds. I. Iben Jr., A. Reninzi, Reidel, Dordrecht, p. 481
Schmidt-Voigt, M., Köppen, J., 1987, A&A 174, 223
Schönberner, D., 1979, A&A 79, 108
Schönberner, D.: 1983, ApJ 272, 708
Schönberner, D., 1987, in *Late Stages of Stellar Evolution*, ed.s S. Kwok & S.R. Pottasch, Reidel, Dordrecht, p. 337
Schönberner, D., 1993, in *Planetary Nebulae*, IAU Symp. 155, eds. R. Weinberger, A. Acker, Kluwer, Dordrecht, p. 415
Schönberner, D., Blöcker, T., 1993, in *Luminous High Lattitude Stars*, ed. D. Sasselov, ASP Conference Series, Vol. 45, p. 337
Schönberner, D., Tylenda, R., 1990, A&A 234, 439
Sweigert, A.V., Greggio, L., Renzini, A., 1990, ApJ 364, 527
van der Veen, W.E.C.J., Habing, H.J., Geballe, T.R., 1989, A&A 226, 108
Vassiliadis, E., Wood, P.R., 1993, ApJ 413, 641
Vassiliadis, E., Wood, P.R., 1994, ApJS 92, 125
Weidemann, V.: 1987, A&A 188, 74
Wood, P.R., Faulkner, D.J., 1986, ApJ 307, 659
Wood, P.R., Zarro, D.M.:1981, ApJ 247, 247
Zalewski, J., 1994, private communication

This article was processed by the author using Springer-Verlag LaTeX A&A style file version 3.